

A SIMPLIFIED MODEL OF A CLIMBING FILM EVAPORATOR AND ITS PRACTICAL APPLICATION

¹SD PEACOCK AND ²M STARZAK

¹*Sugar Milling Research Institute, University of Natal, Durban, 4041*

²*University of Natal, King George V Avenue, Durban, 4001*

Abstract

A complex mathematical model of a climbing film evaporator, based on rigorous material and heat balances, was developed by Peacock and Starzak (1996). Empirical correlations were used to describe the heat transfer and hydrodynamics within the evaporator tubes, taking account of the different regimes of heat transfer and fluid flow encountered during evaporation. The model was used to modify the existing nucleate boiling heat transfer correlation by fitting experimental data from the Felixton (FX) pilot plant climbing film evaporator. Because of the complexity of the model and the extensive computational time required for solution, the amount of data correlated had to be severely limited. In order to overcome this difficulty, a new simplified model is proposed. This was found to be an acceptable approximation of the complex model, giving very similar solutions under all of the process conditions tested. The simplified model was used in the study of three useful practical applications: determination of the effect of juice flow rate on the overall heat transfer coefficient in a climbing film evaporator, influence of juice recycle on evaporator performance, and optimal evaporator tube configuration for the performance of a given heat transfer duty. The results of these studies suggest that, while the model cannot accurately predict evaporator performance, it can be used to predict the general trends in evaporator behaviour. Further work will need to be done to discover the reason for the discrepancies between the model predictions and experimental results.

Keywords: climbing film evaporator, modelling, Felixton

Introduction

In recent years, much work has gone into the study of climbing film evaporators in the South African sugar industry, in terms of both mathematical modelling and experimental study. Most of the experimental work has focussed on the FX pilot plant climbing film evaporator (Walthew *et al.*, 1995; Walthew and Whitelaw, 1996) and is discussed elsewhere. It is the mathematical modelling of climbing film evaporators which is of concern here.

Recently, Peacock and Starzak (1996) developed a complex mathematical model of a climbing film evaporator. Using rigorous material and heat balances, six ordinary differential equations (ODEs) were developed to describe the climbing film evaporator system. While four of these ODEs could be solved

analytically, the remaining two equations were strongly coupled and nonlinear, requiring numerical solution. A shooting method based on the Newton-Raphson technique was used to solve the resulting two point boundary value problem, using empirical correlations to describe the two phase hydrodynamic and heat transfer phenomena occurring within the evaporator tubes. Verification of the complex model using experimental data from the FX pilot plant evaporator indicated that the model under-predicted the heat transfer actually occurring in the pilot evaporator. In order to rectify this problem, an attempt was made to modify appropriately the nucleate boiling heat transfer correlation in the model to yield more accurate results by fitting it to the experimental data from the pilot plant evaporator. However, because of the complexity of the model and the extensive computational time required for solution, this process was found to be extremely difficult. In order to circumvent these difficulties, it was decided to develop a simplified model of the climbing film evaporator based on linearisation of the original ODEs, which could be integrated analytically.

Although the original intention behind the idea of a simplified evaporator model was to apply it to the modification of the saturated nucleate boiling correlation, there are some simple, but still important, applications as well. Three of these are discussed in this study.

Model development

Of the six ODEs describing the climbing film evaporator system, the two strongly coupled, nonlinear equations requiring numerical solution were those resulting from the overall enthalpy balance and the momentum balance. These equations can be presented in the following general mathematical form:

$$\frac{dh}{dz} = F(z, h, p) \qquad \frac{dp}{dz} = G(z, h, p)$$

It should be noted that these complex functions F and G depend not only on enthalpy flow (h) and pressure (p), but also on the independent variable of the model, the distance (z) traveled up the evaporator tube. This is a result of the changes in the two phase flow and heat transfer characteristics which take place as the fluid to be concentrated moves up the tube. Moreover, as different heat transfer correlations are used in each of the individual heat transfer regimes in the evaporator tube (non-boiling zone, subcooled nucleate boiling zone and saturated

nucleate boiling zone), some of the changes in F and G at the transition points between these zones are discontinuous. Thus the characters of the two functions, F and G, change as the tube is traversed. It was decided to emphasise the discontinuities in these functions by using piece-wise representations of F and G, with individual segments being valid in each of the respective zones of boiling. In other words, each of the two functions can be represented by three sub-functions, each being applicable in only one of the three heat transfer zones and independent of distance, z. This concept can be expressed mathematically as:

$$F(z,h,p) = \begin{cases} F1(h,p), & 0 < z < z_{12}, \text{ non-boiling zone} \\ F2(h,p), & z_{12} < z < z_{23}, \text{ subcooled boiling zone} \\ F3(h,p), & z_{23} < z < L, \text{ saturated boiling zone} \end{cases}$$

where z_{12} and z_{23} are the transition points between zones. A similar representation can be given to $G(z,h,p)$. Obviously, this piece-wise nature of the governing ODEs complicates the process of their linearisation, with each of the three heat transfer zones requiring separate treatment.

The non-boiling zone

With the application of some generally acceptable simplifying assumptions, such as:

- negligible heat transfer resistance on the condensate side
- negligible heat transfer resistance due to the tube wall
- constant wall temperature T_w in this zone, being the same temperature as the condensing steam T_s (this is, in fact, a direct result of the two above assumptions)
- negligible acceleration term in the momentum balance
- constant physical properties of the juice

the two functions characterising the non-boiling zone, $F1(z,h,p)$ and $G1(z,h,p)$, become linear without the requirement of any special linearisation technique. $F1$ and $G1$ can then be independently integrated to give an exponential distribution of the local juice temperature:

$$T^j_L(z) = T_s - (T_s - T_{L0}) \exp\left(-\frac{\pi \cdot D_{in} \cdot \alpha_L}{c_p} \cdot z\right)$$

and a linear distribution of the local pressure:

$$p^j(z) = p_0 - (\rho_L \cdot g - \left[\frac{dp}{dz}\right]_{friction}) \cdot z$$

While the exact mathematical results of this analytical integration are not important to this discussion, they are presented here due to their usefulness in studying such phenomena as the effect of feed juice temperature on the length of the non-boiling zone.

The subcooled and saturated nucleate boiling zones

The F and G sub-functions for the two boiling zones (subcooled and saturated nucleate boiling) are much more complicated than those for the non-boiling zone, and simple physical arguments

like those used above are insufficient to linearise them. A purely formal linearisation technique, such as a truncated Taylor expansion about an arbitrarily chosen point (h^*, p^*) , can be used. Alternatively, as F and G are functions of two variables, linearisation can be performed by approximating some actual known values of the function with a planar representation over a certain range of h and p values (the three dimensional equivalent of fitting a straight line to a set of points in two dimensions). In this study, this second method of linearisation was used, as it predicts more realistic values of F and G over the entire (h, p) domain of interest, rather than just about an arbitrary (h^*, p^*) point.

Examples of the surfaces representing F and G for both the subcooled and saturated nucleate boiling regimes have been numerically generated and are displayed in Figures 1 and 2. The surfaces $F2$ and $G2$, shown in Figure 1, are fairly planar and can be well represented by their linearised planar counterparts. On the other hand, inspection of the surfaces $F3$ and $G3$ in Figure 2 shows that $G3$ is highly nonlinear over a certain region of the graph, exhibiting a large degree of curvature near the edge of the graph representing the transition from subcooled boiling to saturated boiling. However, by performing some numerical experiments, it was found that this initial phase of saturated nucleate boiling had a negligible impact on the overall performance of the evaporator, and that a good linear approximation of this surface could be obtained.

Model solution

Once the linearised forms of F and G have been obtained, it becomes possible to solve the linearised system of ODEs analytically, yielding explicit relationships for enthalpy flow (or temperature, in the case of the non-boiling zone) and pressure in each of the three heat transfer zones. Full details of the model formulation and solution will become available (Peacock, 1997-98, in preparation).

Comparison with the complex model

The simplified model was validated by comparing the results of several tests under differing operating conditions against those obtained from the complex model under the same conditions. Some selected graphical results from two such comparative tests are displayed in Figures 3 and 4, with the results from the complex model being shown as the solid lines in the figures and the results of the simplified model being displayed as the broken lines.

The plots labelled (a) in Figures 3 and 4 show the juice temperature profile as the evaporator tube is traversed. Under the conditions used in these examples, the juice reached its boiling point very rapidly upon entering the tubes. Once saturated nucleate boiling has been initiated, the juice temperature remains fairly constant, decreasing slightly as the tube is traversed due to the reduction of hydrostatic head with height up the tube.

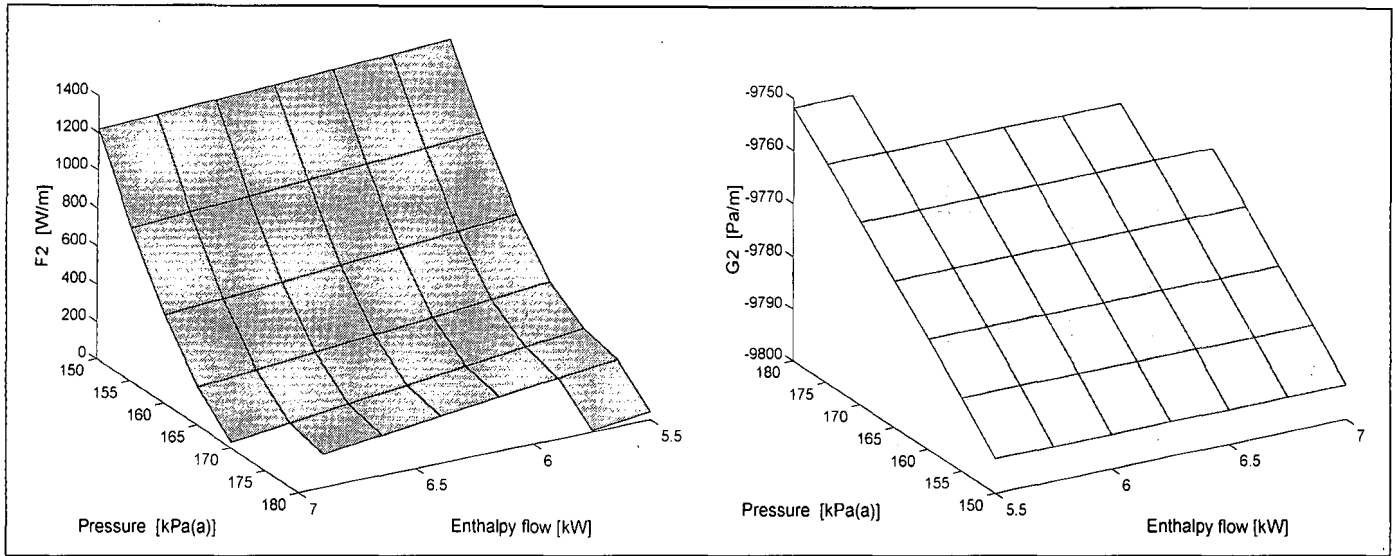


Figure 1. Examples of the F and G surfaces for the subcooled nucleate boiling regime.

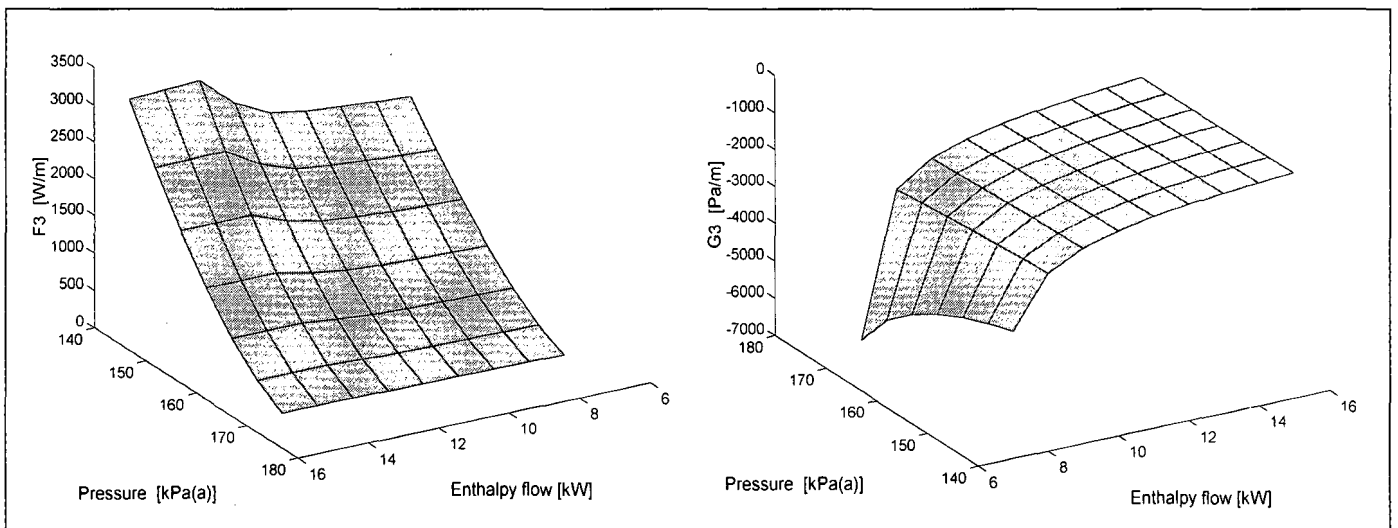


Figure 2. Examples of the F and G surfaces for the saturated nucleate boiling regime.

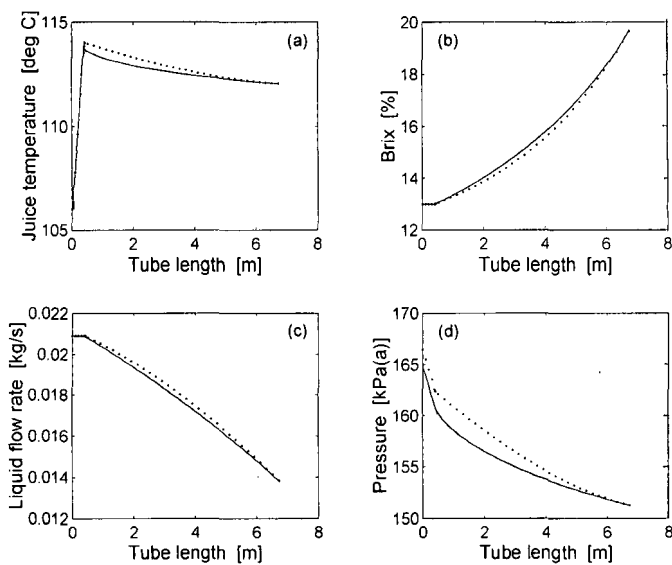


Figure 3. Selected graphical results from model simulations.

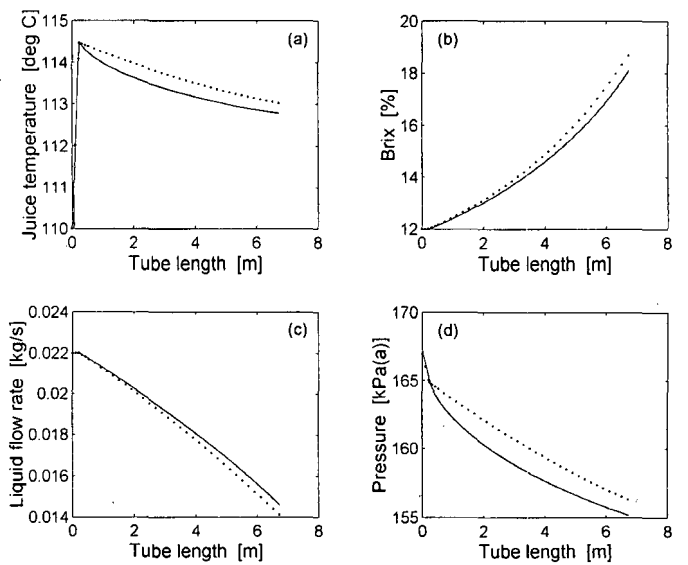


Figure 4. Selected graphical results from model simulations.

The plots labelled (b) show the brix profile of the juice as it moves through the evaporator tubes. It can be clearly seen that the simplified model better approximated the complex model under the conditions prevailing for the example in Figure 3. A slight error in the predicted syrup brix is evident in Figure 4(b).

The plots labelled (c) in Figures 3 and 4 display the liquid phase flow rate through the evaporator tube. As vapour is formed, the liquid phase flow rate drops proportionately. As the liquid phase flow rate and brix are intimately related, the error evident in Figure 4(b) is also apparent in Figure 4(c).

Plots 3(d) and 4(d) show the local pressure profiles along the evaporator tubes. Once again, it is clear that the example in Figure 3 was more accurately approximated by the simplified model than that in Figure 4.

While minor differences between the results are apparent, it can be seen that the simplified model is a good representation of the more exact, complex model.

Application 1: The effect of juice flow rate

The feed juice flow rate to climbing film evaporators is of critical importance to their efficient operation. Tests performed using the FX pilot plant evaporator have described the effect of juice flow rate on evaporator performance (Walthew and Whitelaw, 1996) and the results of some of these tests are shown in Figure 5. In order to confirm the experimental observations, the simplified evaporator model was used to study the effect of feed juice flow rate on the overall heat transfer coefficient of a climbing film evaporator. The operating conditions used in the study are shown in Table 1. Three different tube diameters (38,40, 48,36 and 71,60 mm inner diameters) were used, with feed juice flow rates varying between 0,5 and 3 kg/min/tube. The results of the model simulations are shown in Figure 6.

Table 1
Operating conditions for the study of feed juice flow rate.

| | |
|-----------------------------|-------|
| Number of tubes | 5 000 |
| Tube length (m) | 6,73 |
| Feed brix (%) | 12 |
| Feed purity (%) | 85 |
| Feed juice temperature (°C) | 110 |
| Steam pressure (kPa[a]) | 200 |
| Vapour pressure (kPa[a]) | 155 |

Figure 6 confirms the general trend of the experimental data (obtained using 48,36 mm inner diameter tubes in the FX pilot plant evaporator - refer to Figure 5). However, the feed juice flow rate at which the step increase in overall heat transfer coefficient (HTC) occurs, as predicted by the model, is different to that obtained experimentally. The reason for this difference is not yet known, and more work will be required to identify its

source. As expected, the flow rate at which the step increase in overall HTC occurs increases with tube diameter. This is due to the increase in cross sectional area available for flow within the tube with increasing tube diameter; in a small diameter tube, a lower flow rate is required for good wetting of the tube surface than in a large diameter tube. The step change in heat transfer coefficient is not visible on the curve for the 71,60 mm internal diameter (ID) tube, as it probably occurs at a flow rate higher than those studied here. Using the model to determine the effect of tube diameter on HTC showed that, for each feed juice flow rate, an optimal tube diameter exists which maximises the HTC. At the typical feed juice flow rates used in the South African sugar industry, tubes of inner diameter 48,36 mm would appear to be a good choice.

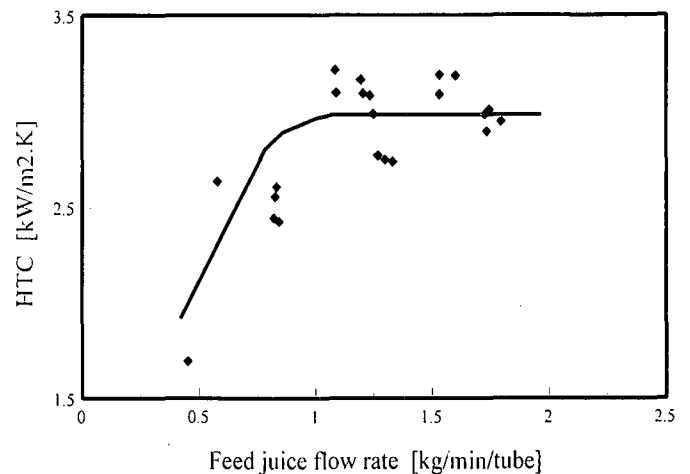


Figure 5. Experiment observations of the effect of juice flow rate on HTC.

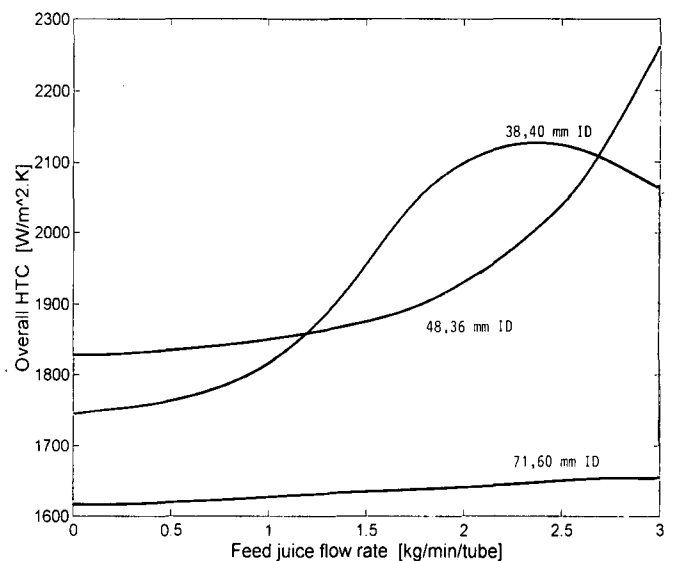


Figure 6. Effect of juice flow rate on evaporator performance.

Walthew and Whitelaw (1996) showed that a low feed juice flow rate limits the maximum attainable HTC for a climbing film evaporator by limiting the water available for evaporation. They also showed that the asymptotic fouling factor decreased

with increasing feed juice flow rate. These factors, along with the experimental data and the results of this study, indicate that climbing film evaporators should be operated so as to achieve a consistently high feed juice flow rate.

Application 2: The effect of juice recycle

Problem formulation

In general, a conflict of interests exists in the process of heat transfer within a climbing film evaporator. A relatively low liquid feed flow rate per tube is desirable to ensure a reasonable juice residence time within the evaporator. This allows for a high degree of evaporation to take place. By contrast, low liquid flow rates result in laminar flow conditions within the evaporator tubes, leading to very poor convective heat transfer coefficients¹. In the subcooled and saturated nucleate boiling zones, the nucleate boiling mechanism dominates the heat transfer, with very little contribution to the overall heat transfer coefficient due to convection. As nucleate boiling is not very sensitive to flow rate, the effect of low flow rates on heat transfer in these zones is small. However, laminar flow conditions dramatically affect the length of the non-boiling zone, where convective heat transfer dominates. As any increase in the length of the non-boiling zone results in a shortening of the length of the tube available for the more efficient boiling zones, overall heat transfer is negatively affected.

Two techniques can be used to eliminate this conflict of interests. The first of these is adequate preheating of the feed juice to the evaporator to ensure the onset of nucleate boiling as soon as possible after the juice enters the evaporator tubes, thus effectively eliminating the poor heat transfer non-boiling zone. A preliminary mathematical study of the effect of preheating on the length of the non-boiling zone has been performed (Peacock, 1996). The second technique involves the recycling of a portion of the liquid phase leaving the evaporator back to the feed inlet in order to improve the system hydrodynamics.

While increasing the flow rate per tube results in more efficient convective heat transfer, the overall effect of recycling on evaporator performance is more complex. As a result of the addition of higher brix juice from the evaporator outlet, the physical properties of the juice stream fed to the evaporator, such as density and viscosity, increase, negatively affecting overall performance. The combined result of these effects can not be intuitively determined for any given system. It was thus decided to apply the simplified evaporator model to study the effect of recycling on evaporator performance more closely.

¹Very low juice flow rates to climbing film evaporators can also result in partial tube 'dry-out' at the top end of the tubes, with the consequences of a significant decrease in the overall heat transfer and greatly accelerated tube fouling. In this study, the effect of dry-out on evaporator performance was not studied, and the evaporator operating conditions used were chosen so as to avoid the occurrence of dry-out at the end of the tube, while still being representative of general process conditions in the South African sugar industry.

Recycling for process stability

Recycling of juice during evaporation results in more than just enhanced convection, with benefits also achieved in terms of process stability. The damping effect of recycling enables minor feed juice fluctuations to be eliminated easily, resulting in more steady evaporator operation. The benefits of steady operation and consistent juice flow, in terms of the elimination of the possibility of tube 'dry-out' and the mitigation of evaporator fouling, are significant and it is predominantly for these benefits that some South African sugar mills have installed juice recycle lines in their climbing film evaporators, not for the enhancement of convection. Nonetheless, it is important to be able to evaluate the effect of recycling on evaporator performance, regardless of the reasons for its use.

Model application and results

For this study, the operation of a specific evaporator was simulated at a given set of feed conditions, at several fixed values of the recycle fraction (defined as the fraction of the liquid phase from the outlet of the evaporator which is returned to the inlet). A diagram of the evaporator system used is displayed in Figure 7. The outlet brix of the product stream from the evaporator was used as the measure of system performance. The operating conditions used for the study are shown in Table 2, and the results of the investigation are shown in Figure 8.

Table 2
Operating conditions for the study of evaporator recycling.

| | |
|--------------------------------|-------|
| Tube inner diameter (mm) | 48,36 |
| Tube outer diameter (mm) | 50,80 |
| Number of tubes | 5 000 |
| Tube length (m) | 6,73 |
| Throughput (m ³ /h) | 400 |
| Feed brix (%) | 12 |
| Feed purity (%) | 85 |
| Feed juice temperature (°C) | 110 |
| Steam pressure (kPa[a]) | 200 |
| Vapour pressure (kPa[a]) | 155 |

It can be seen that optimisation of the recycle fraction *per se* is not possible. As predicted, the effect of recycling on syrup brix is a complex combination of the enhanced system hydrodynamics and the negative effects of the higher average density and viscosity in the tubes. At low recycle fractions, the negative physical property effects and the positive hydrodynamic effects appear to balance each other, with no real effect on evaporator performance being observed due to recycling. At higher recycle fractions, the hydrodynamic advantages of the recycling start to affect the evaporator performance, improving the outlet syrup brix. It must be noted that the recycle fractions required to confer

significant performance enhancement benefits are high (of the order of 60-70%), and some experimental work will be needed to confirm this result.

The results of this study confirm the general opinion that recycling in climbing film evaporators should be performed for process stability and fouling control reasons, not for heat transfer performance enhancement. It is clear that recycle fractions of 50% or less will have no observable effect on evaporator performance (excluding considerations of 'dry-out'). At higher recycle fractions, a small performance benefit may be obtained, but at the expense of recycling large quantities of liquid.

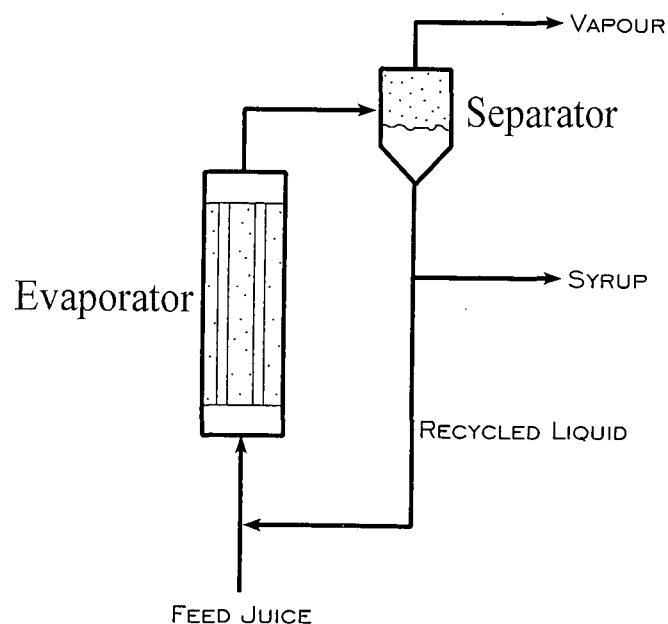


Figure 7. Diagram of the evaporator system for the study of juice recycling.

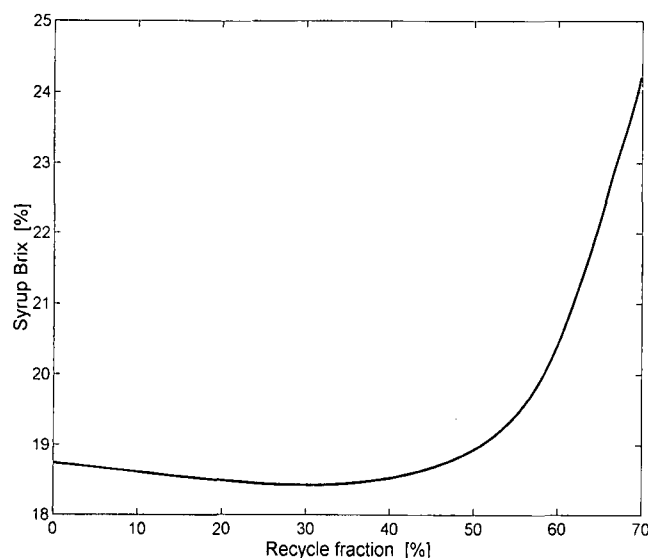


Figure 8. Effect of juice recycling on outlet syrup brix.

Application 3: Tube configuration optimisation

For the purposes of climbing film evaporator design, it is desirable to know the required surface area for the performance of a specific heat transfer duty under a given set of operating conditions. A problem of particular current interest to the South African sugar industry is the effect of different tube diameters on evaporator performance. The simplified climbing film evaporator model was thus used to evaluate the effects of different tube diameters and numbers of tubes on the required surface area for the achievement of a specific heat transfer duty (in fact, with a fixed tube diameter and number of tubes, evaluating the required surface area for heat transfer reduces to the problem of evaluating the required evaporator tube length, as this is the only surface area parameter not already specified).

The operating conditions used in this application are displayed in Table 3. Three different tube diameters were evaluated (38,40, 48,36 and 71,60 mm inner diameters), with numbers of tubes ranging from 3 000 to 8 500 tubes per evaporator. A summary of the model results is displayed in Figure 9. With a fixed volumetric throughput for the evaporator, as in this case, specifying the tube diameter and number of tubes uniquely fixes the juice flow velocity per tube. As the juice flow velocity allows more meaningful comparisons between evaporators of differing tube sizes than the number of tubes per evaporator, this parameter has been used along the x-axis in Figure 9. Detailed results of the model simulations are shown in the Appendix. When interpreting the results of this application, it must be remembered that the syrup brix from the evaporator remains fixed, with the tube length being varied to obtain this desired syrup brix. This makes comparison of the results with classical wisdom (relating to evaporators of fixed tube length) difficult.

Table 3

Operating conditions for the study of tube diameter effects.

| | |
|--------------------------------|-----|
| Throughput (m ³ /h) | 400 |
| Feed brix (%) | 12 |
| Required syrup brix (%) | 25 |
| Feed juice temperature (°C) | 110 |
| Steam pressure (kPa[a]) | 200 |
| Vapour pressure (kPa[a]) | 155 |
| Feed purity (%) | 85 |

From Figure 9, it can be seen that the required surface area for the performance of a given heat transfer duty is fairly sensitive to the juice flow velocity. The results in Figure 9 imply that, in the design of climbing film evaporators, it is not only the overall surface area required which is important, but also the actual dimensions of the evaporator. It is better, in terms of minimisation of installed heat transfer area, to utilise many

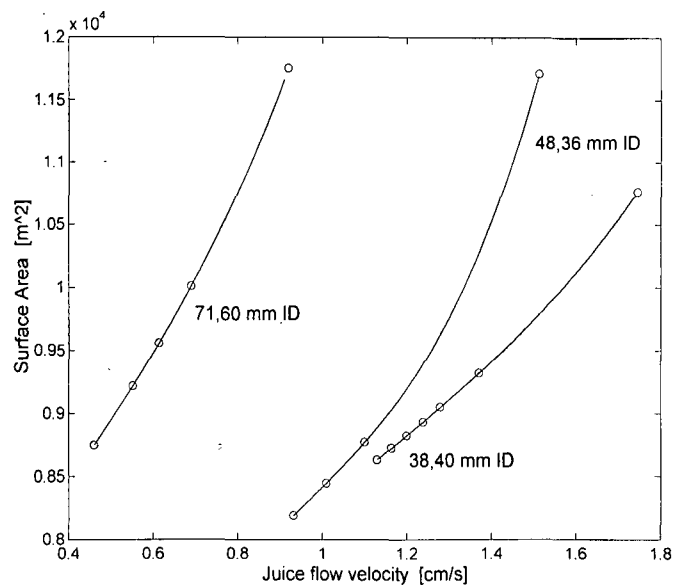


Figure 9. Required evaporator surface area for a given heat transfer duty as a function of tube size and number of tubes.

(relatively) short tubes in a climbing film evaporator, thereby keeping the juice flow velocity near the optimal point, than to use fewer, long tubes².

While the graph shows a monotonic decrease in required surface area with decreasing juice flow velocity, this trend cannot continue unabated, and it is expected that an optimal juice flow velocity will exist for each tube size which results in a minimisation of the required surface area for the performance of the given heat transfer duty.

The optimal juice flow velocity can be seen to decrease with increasing tube diameter. This result is not unexpected in that the larger the tube diameter (and, consequently, the larger the volume of liquid within the tube not in close contact with the tube wall), the longer the residence time required by the juice for good evaporation. However, it would appear that tube diameter does not play a major role in the performance of properly designed climbing film evaporators, as the optimal surface areas which can be obtained for each of the three tube diameters are similar. More work will need to be done to confirm this conclusion.

Most climbing film evaporators in the South African sugar industry use 48,36 mm internal diameter (ID) tubes, and operate at juice flow velocities of around 1 cm/s. Figure 9 demonstrates

²With reference to the table in the Appendix, it can be seen that 'short tubes' refer to tubes of 6-9 m in length, while 'longer tubes' refer to tubes with lengths greater than 9m. The typical climbing film evaporator configurations used in the South African sugar industry conform to this recommendation.

³As the model tends to under-predict the heat transfer actually occurring in climbing film evaporators (Peacock and Starzak, 1996) the required surface area predicted by the model under these conditions is higher than that actually used in the industry.

⁴DC Walthew, Sugar Milling Research Institute, Durban (1997).

the reason for this choice of operating conditions³. However, the results of the simplified climbing film evaporator model do not take into account the effects of evaporator operating conditions on fouling, nor the effects of fouling on heat transfer. These effects are critical to the operation of industrial evaporators. Tests using the FX pilot plant evaporator, as discussed in Application 1, have shown that it is important that climbing film evaporators be operated above a specific flow rate (about 1,2 kg/s/tube for 48,36 mm ID tubes) in order to avoid tube dry-out and decreased performance due to high rates of fouling (⁴personal communication). This fact should be borne in mind when designing climbing film evaporator systems and steps should be taken to ensure that the juice flow to the evaporator never drops below this critical value (possibly using juice recycling to achieve a consistent flow rate through the tubes). It may thus be safer to err on the side of high juice flow velocities when designing a climbing film evaporator, sacrificing some heat transfer performance in the interests of fouling mitigation.

Conclusions

A new simplified model of a climbing film evaporator is proposed. The simplified model was found to be an acceptable approximation of the more complex model, described previously by Peacock and Starzak (1996), under all of the process conditions tested. The application of the model to the study of three useful practical problems was discussed.

In Application 1, the model was used to study the effect of feed juice flow rate on the overall heat transfer coefficient of a climbing film evaporator. The results obtained were found to corroborate the general trends observed experimentally, using the FX pilot plant evaporator, although showing quite large discrepancies with the actual numerical results of the experiments. More work is required to evaluate the causes of these discrepancies.

Studying the effect of juice recycling on climbing film evaporator performance in Application 2 confirmed that, at recycle fractions of 50% or less, recycling has no significant effect. At higher recycle fractions a performance benefit was observed, but practical considerations may make the use of such high recycle ratios undesirable.

In Application 3, the simplified model was applied to the study of the effects of tube diameter and numbers of tubes on the performance of climbing film evaporators. The surface area required for the achievement of a specified heat transfer duty was evaluated at three different tube diameters, with differing numbers of tubes. It was found to be better to use many relatively short tubes than fewer, longer tubes in the design of climbing film evaporators. The results were found to confirm the conventional wisdom of the South African sugar industry with regard to evaporator tube configuration.

REFERENCES

- Peacock, SD (1996). The optimisation of feed juice temperature for climbing film evaporators - a preliminary study. Sugar Milling Research Institute Technical Note No. 49/96. 7 pp.
- Peacock, SD (1997-98). The mathematical modelling of climbing film evaporators. MSc Eng (Chem) Thesis, University of Natal (in preparation).
- Peacock, SD and Starzak, M (1996). Modelling of climbing film evaporators. *Proc S Afr Sug Technol Ass* 70: 213-220.
- Walthew, DC and Whitelaw, RW (1996). Factors affecting the performance of long tube climbing film evaporators. *Proc S Afr Sug Technol Ass* 70: 221-224.
- Walthew, DC, Whitelaw, RW and Peacock, SD (1995). Preliminary results from a long tube climbing film pilot plant evaporator. *Proc S Afr Sug Technol Ass* 69: 132-137.

NOMENCLATURE

| | |
|-----------------------------|---|
| c_p | Average specific heat capacity of the juice in the non-boiling zone of the tube [J/kg.K]. |
| $(dp/dz)_{\text{friction}}$ | Pressure drop per metre of tube due to wall friction [Pa/m]. |
| D_{in} | Inner diameter of the evaporator tube [m]. |
| F | Complex function representing the right hand side of the ordinary differential equation resulting from the overall enthalpy balance in the evaporator tube. |
| F_1 | Sub-function representing F in the non-boiling zone of the tube. |
| F_2 | Sub-function representing F in the subcooled nucleate boiling zone of the tube. |
| F_3 | Sub-function representing F in the saturated nucleate boiling zone of the tube. |
| g | Gravitational acceleration [m/s^2]. |
| G | Complex function representing the right hand side of the ordinary differential equation resulting from the momentum balance in the evaporator tube. |
| G_1 | Sub-function representing G in the non-boiling zone of the tube. |
| G_2 | Sub-function representing G in the subcooled nucleate boiling zone of the tube. |
| G_3 | Sub-function representing G in the saturated nucleate boiling zone of the tube. |
| h | Enthalpy flow in the evaporator tube [W]. |
| h^* | Enthalpy flow at the arbitrarily chosen (h^* , p^*) point of a truncated Taylor expansion [W]. |
| L | Tube length [m]. |
| p | Pressure [Pa]. |
| p^* | Pressure at the arbitrarily chosen (h^* , p^*) point of a truncated Taylor expansion [Pa]. |
| $p^l(z)$ | Local pressure at point z within the tube, in the non-boiling zone [Pa]. |
| p_0 | Local pressure at the bottom of the evaporator tube (where $z = 0$) [Pa]. |
| $T^l_L(z)$ | Local temperature of the juice at point z within the tube, in the non-boiling zone [$^{\circ}\text{C}$]. |
| T_{L0} | Temperature of the juice entering the bottom of the evaporator tubes (at $z = 0$) [$^{\circ}\text{C}$]. |
| T_s | Steam temperature [$^{\circ}\text{C}$]. |
| T_w | Inner tube wall temperature in the non-boiling zone [$^{\circ}\text{C}$]. |
| z | Distance in the evaporator tube, measured from the bottom of the tubes [m]. |
| z_{12} | Distance in the tube at which the non-boiling zone ceases and the subcooled nucleate boiling zone begins [m]. |
| z_{23} | Distance in the tube at which the subcooled nucleate boiling zone ceases and the saturated nucleate boiling zone begins [m]. |
| α_L | Convective heat transfer coefficient in the non-boiling zone [$\text{W/m}^2\text{.K}$]. |
| ρ_L | Average juice density in the non-boiling zone [kg/m^3]. |

APPENDIX
Detailed results of the model simulations for Application 3.

| Input data | | | | Model results | | |
|--------------------------|--------------------------|-----------------|----------------------------|--------------------------------|------------------------------------|-----------------|
| Inner tube diameter (mm) | Outer tube diameter (mm) | Number of tubes | Juice flow velocity (cm/s) | Surface area (m ²) | Average HTC (kW/m ² .K) | Tube length (m) |
| 38,40 | 42,40 | 5 500 | 1,74 | 10 762 | 1,33 | 16,2 |
| | | 7 000 | 1,37 | 9 322 | 1,54 | 11,0 |
| | | 7 500 | 1,28 | 9 048 | 1,59 | 10,0 |
| | | 7 750 | 1,24 | 8 928 | 1,61 | 9,6 |
| | | 8 000 | 1,20 | 8 819 | 1,63 | 9,1 |
| | | 8 250 | 1,16 | 8 719 | 1,64 | 8,8 |
| | | 8 500 | 1,13 | 8 627 | 1,66 | 8,4 |
| 48,36 | 50,80 | 4 000 | 1,51 | 11 713 | 1,21 | 19,3 |
| | | 5 500 | 1,10 | 8 767 | 1,64 | 10,5 |
| | | 6 000 | 1,01 | 8 444 | 1,70 | 9,3 |
| | | 6 500 | 0,93 | 8 188 | 1,75 | 8,3 |
| 71,60 | 76,10 | 3 000 | 0,92 | 11 753 | 1,22 | 17,4 |
| | | 4 000 | 0,69 | 10 012 | 1,43 | 11,1 |
| | | 4 500 | 0,61 | 9 557 | 1,50 | 9,4 |
| | | 5 000 | 0,55 | 9 220 | 1,56 | 8,2 |
| | | 6 000 | 0,46 | 8 746 | 1,64 | 6,5 |